http://dx.doi.org/10.5012/bkcs.2013.34.7.2105

Catalytic NiO Filter Supported on Carbon Fiber for Oxidation of Volatile Organic Compounds

Jong Ki Sim, Hyun Ook Seo, Myung-Geun Jeong, Kwang-Dae Kim, Young Dok Kim,* and Dong Chan Lim†

*Department of Chemistry, Sungkyunkwan University, Suwon 440-746, Korea. *E-mail: ydkim91@skku.edu*
†Materials Processing Division, Korea Institute of Materials Science, Changwon 641-010, Korea
Received April 2, 2013, Accepted April 20, 2013

Carbon-fiber-supported NiO catalytic filters for oxidation of volatile organic compounds were prepared by electroless Ni-P plating and subsequent annealing processes. Surface structure and crystallinity of NiO film on carbon fiber could be modified by post-annealing at different temperatures (500 and 650 ºC). Catalytic thermal decompositions of toluene over these catalytic filters were investigated. 500 ºC-annealed sample showed a higher catalytic reactivity toward toluene decomposition than 650 ºC-annealed one under same conditions, despite of its lower surface area and toluene adsorption capacity. X-ray diffraction and X-ray photoelectron spectroscopy studies suggest that amorphous structures of NiO on 500 ºC-annealed catalyst caused the higher reactivity for oxidation of toluene than that of 650 ºC-annealed sample with a higher crystallinity.

Key Words : Volatile organic compounds, NiO, Catalytic oxidation

Introduction

Removal of volatile organic compounds (VOCs) has been attracting much attention, due to their high toxicity and malodorous nature.[1] VOCs themselves can cause sick-building syndrome, including irritation of the eye, nose, throat and neurotoxic health problems in indoor environments.[2,3] In addition, some toxic photochemical oxidants and suspended particulate matters can be produced as a result of photochemical reactions of VOCs under light irradiations.[4-6] Many different ways, such as adsorption, pyrolysis, photocatalytic degradation, and catalytic oxidation, have been suggested and investigated for removing VOCs pollutants. Among those, catalytic oxidation of VOCs has been considered as one of the most promising ways due to its high destruction efficiency.[5-9]

Various transition metal-based catalysts (Pt, Pd, MnO, CuO, NiO, *etc.*) have been investigated for the catalytic oxidation of VOCs.[5-8,10-13] So far, noble metal-based catalysts, especially Pt-based ones, are known to be the most active catalyst at low temperature for thermal oxidation of VOCs.[5,6,14] However, their high costs and limited abundance make it difficult to use them in large-scale applications. Thus, noble-metal free catalysts based on other transition metal-oxides (MnO, CuO, Co_3O_4, NiO, *etc.*) have been extensively investigated as alternatives to noble metal catalysts in catalytic oxidation of VOCs for the last decades.[8,10-13,15] For instance, CuO, Co_3O_4, CeO_2 and MnO have been reported to have comparable catalytic activity toward VOCs oxidation with those of noble-metal catalyst.[11,15-18] Lahousse *et al.* reported that γ-MnO_2 could be more catalytically active than other supported-noble-metal catalysts.[19] Recently, it has been suggested that NiO also exhibits catalytic reactivity towards oxidative reactions[20,21] and our previous results on TiO_2/NiO catalytic system also revealed that NiO state can act as active sites for thermal decomposition of toluene.[13]

In the present work, NiO films were deposited on carbon filter consisting of carbon fiber with a mean diameter of 10 μm using electroless plating method and subsequent annealing steps. Use of filter type catalysts is more beneficial than powder catalysts, since filter type can be more easily handled and better recycled. Surface structure and crystallinity of NiO films could be modified by choosing different temperatures for post-annealing processes. Catalytic reactivities of NiO filters (amorphous NiO with mesoporous surface and crystalline NiO with macro porous structure, respectively) for thermal oxidation of toluene were investigated and compared with their toluene adsorption capacities.

Experimental

Sample Preparation. Carbon filter (Toray 060) with a Brunauer-Emmett-Teller (BET) surface area of 0.4 m^2/g was purchased from Toray and used as a substrate. Carbon filters consisting of carbon fibers with a mean diameter of 10 μm were annealed at 700 ºC for 3 h under atmospheric conditions before deposition of thick NiO films. The thickness of the carbon filter was 140 μm. NiO filters were prepared by deposition of NiO films on pre-annealed carbon fiber using electroless Ni-P plating method and subsequent annealing processes. Initially, the surfaces of pre-annealed carbon fibers were activated with Pd catalysts by immersing into the activator solution consisting of $PdCl_2$ (99%, Samchun Chemical, 0.01 g/L), HCl (35.0-37.0%, Samchun Chemical, 3 mL/L) and HF (48.0-51.0%, JT Baker chemicals, 5 mL/L) for 10 min at room temperature. The activated samples were washed with distilled water, and then subsequently dipped into the electroless Ni-P plating solution for 10 min at 100 ºC with a vigorous stirring. The electroless Ni-P plating

solution contained SX-A (Uyemura & Co, Ltd, 56 mL/L) and SX-M (Uyemura & Co, Ltd, 100 mL/L). After Ni-P plating process, samples were rinsed with distilled water and dried at room temperature. Finally, two different NiO filters supported by carbon fibers were prepared by 1 h of post-annealing at 500 and 650 °C, respectively, under atmospheric conditions.

Characterization. The surface morphology of each NiO filter annealed at 500 and 650 °C, respectively, was analyzed using scanning electron microscopy (SEM, JEOL, JSM 7500F). Surface states and crystallinities of two NiO filers (500 and 650 °C-annealed ones) were examined using X-ray photoelectron spectroscopy (XPS) and X-ray diffraction (XRD), respectively, before toluene oxidation. XPS analysis were performed in an ultrahigh-vacuum system (~3×10^{-10} torr) equipped with a concentric hemispherical analyzer (CHA, PHOIBOS-Hsa3500, SPECS) and a dual Al/Mg X-ray source. XPS spectra were taken at room temperature using a Mg Kα irradiation (1253.6 eV). XRD pattern of each sample was obtained using a X-ray diffractormeter (RIFAKU, UltimaIV) with a Cu Kα (0.15406 nm) radiation. The operating condition of XRD was 30 kV and 40 mA and scanning rate was 2°/min.

Toluene Adsorption Experiments. Toluene adsorption capacity of each NiO filter annealed either at 500 or 650 °C was examined in a vacuum reactor (~8.0×10^{-8} torr) at room temperature. Detailed descriptions of experimental set-up for toluene adsorption experiments can be found elsewhere.[22] Each sample with a lateral size of 2 × 2 cm^2 was placed in the vacuum reactor and then sample surface was exposed to a gas mixture of N_2 (80 mtorr) and toluene (5 mtorr). Change in the relative mass intensity of toluene with respect to N_2 was measured by leaking small amount of the gas from the reactor to the analysis chamber equipped with a quadrupole mass spectrometer (QMS) every 5 minutes.

Thermal Oxidation of Toluene Experiments. Catalytic oxidation of toluene over NiO filters was carried out using a flow type quartz reactor equipped with online gas-chromatography (GC, Agilent-6890N) set-up. Intensity of each gas was detected by flame ionization detector (FID) with a methanizer. The rounded sample with 20 mm of diameter was vertically placed into the quartz reactor (inner diameter: 20 mm, length: 300 mm) and its surface was outgassed at 450 °C for 1 h with a flow of dry air (5 mL/min) before reaction. After pre-treatment, temperature of the reactor was decreased to room temperature within 1 h, and then re-increased to 100 °C within 10 min. The 100 °C of temperature was maintained during saturation. After the temperature was reached at 100 °C, valve of toluene bottle was open and about 80 ppm of toluene gas was injected into flow. Gas flow of a mixture of carrier gas and toluene was stabilized during 5 h. After the mixture gas flow was saturated, the temperature of reactor was increased from 100 to 400 °C with a heating rate of 1 °C/min. The catalytic oxidation of toluene over NiO filter was studied with an increase of temperature. During all the process, dry air with a mass flow of 5 mL/min was used as a carrier gas and temperature of toluene bottle was kept at 30 °C. Temperature of the reactor was controlled and monitored by a furnace equipped with a K-type thermocouple.

Results and Discussion

Figure 1 shows morphological SEM images of several NiO filters annealed at different temperatures (from 350 to 900 °C) under atmospheric conditions after electroless Ni-P plating processes. The surface morphology was dependent upon annealing temperatures. The surface of 350 °C-annealed sample was covered with relatively flat NiO film (Fig. 1(a)). However, the relatively flat surface of NiO film was converted into rippled structures with nanopores (50-400 nm) when the sample was annealed at higher temperatures (Fig. 1(b)-(g)). The nanopores on the surface of sample annealed at the highest temperature of 900 °C were clogged. Also, combustion of carbon fiber made the NiO filters fragile over 650 °C.

We selected two different samples which were annealed at 500 and 650 °C respectively, because these two samples showed significant differences in surface morphology, inner structure and pore size. Surface states and crystallinities of these two different samples were further characterized using XPS (Fig. 3) and XRD (Fig. 4), respectively. Two oxidic Ni states (for Ni $2p_{3/2}$, NiO at 853.4 eV and $Ni(OH)_2$ at 855.4

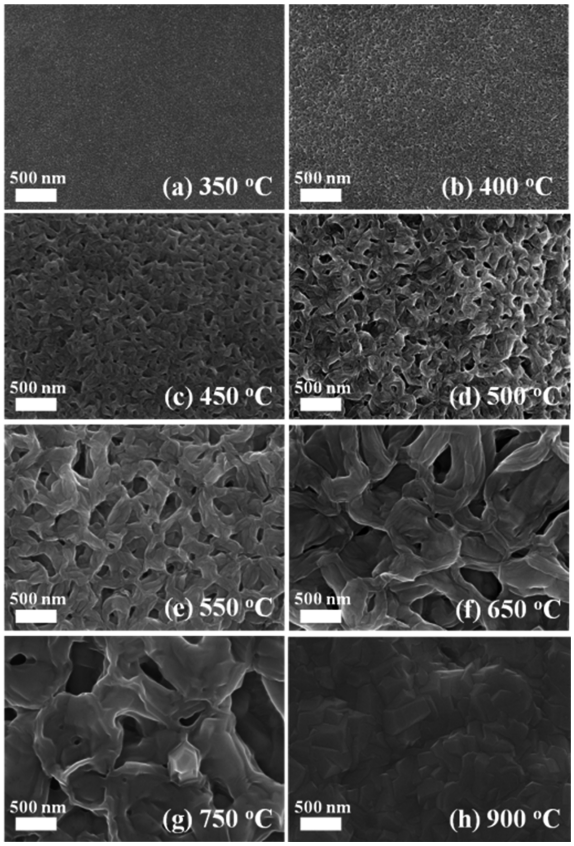

Figure 1. Morphological SEM images of NiO filters annealed at (a) 350 °C, (b) 400 °C, (c) 450 °C, (d) 500 °C, (e) 550 °C, (f) 650 °C, (g) 750 °C and (h) 900 °C are displayed.

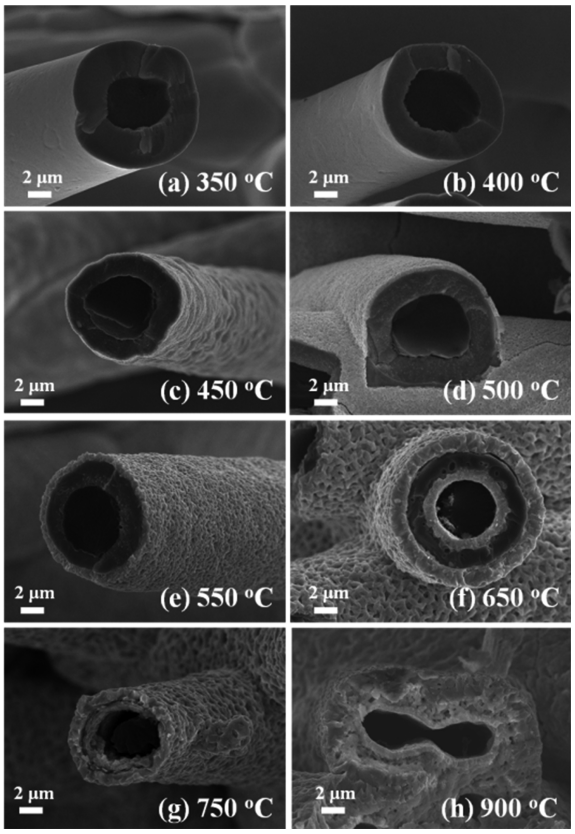

Figure 2. Cross-sectional SEM images of NiO filters annealed at (a) 350 °C, (b) 400 °C, (c) 450 °C, (d) 500 °C, (e) 550 °C, (f) 650 °C, (g) 750 °C and (h) 900 °C are shown.

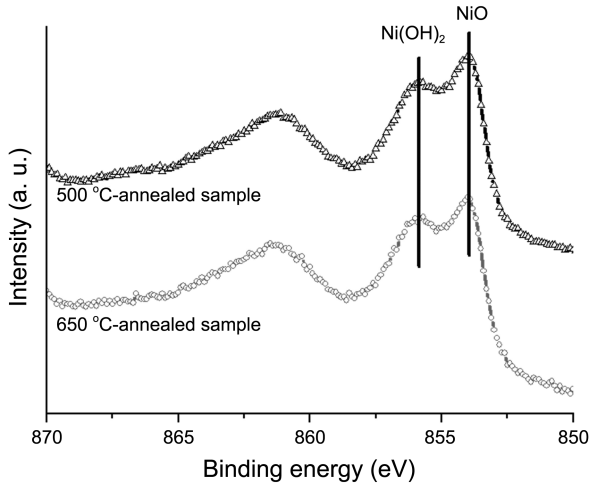

Figure 3. Ni 2p core-level XPS spectra of 500 and 650 °C-annealed NiO filters are compared.

eV) were found in Ni 2p core-level XPS spectra,[13,23,24] whereas any significant peak corresponding to Ni_xP_y state (around at 852.1-852.9 eV) was not observed in the Ni 2p region for both cases (500 and 650 °C-annealed samples) (Fig. 3).[25-27] In addition, any noticeable peak around at 129.5 eV (Ni_xP_y state) could not be found in the P 2p region (Fig. 2 b),[25-27] implying that Ni_xP_y species on the surfaces of both samples were oxidized into the oxidic-Ni species upon post-annealing processes.

Table 1. Surface atomic ratios (%) of 500 and 650 °C-annealed NiO filters determined from XPS data are summarized

	Surface Atoms (%)			
	O 1s	C 1s	Ni 2p	P 2p
500 °C-annealed sample	51.880	26.940	21.179	-
650 °C-annealed sample	48.497	33.220	17.317	0.898

However, very small amount of P species on the surface was still observed in the P 2p core-level XPS spectrum of 650 °C-annealed sample (Table 1), indicating the presence of oxidized P impurities (*e.g.* P_2O_3) in small amounts.[24,28] It is important to mention that these oxidized P species on the surface of 650 °C-annealed samples were found to have no significant effects on catalytic behavior in the present work. The oxidized P impurities on surface of 650 °C-annealed sample disappeared after toluene oxidation up to 450 °C in P 2p XPS spectra which induced no alteration in catalytic activity.

The crystallinities of two NiO filters annealed at 500 and 650 °C, respectively, were investigated using XRD (Fig. 4). XRD analysis indicated that these two NiO films (500 and 650 °C-annealed samples) had different crystalline phases (Fig. 4); the presence of crystalline NiO was pronounced in the XRD spectrum of 650 °C-annealed sample,[29,30] whereas only very small XRD peaks of crystalline NiO phase could be observed in the XRD data of 500 °C-annealed one, indicating that the NiO at 500 °C was amorphous. In contrast to the XPS results where any noticeable peak due to Ni_xP_y state was not found, multiple peaks from 42° to 57° related to various Ni_xP_y states were observed in the XRD patterns of both samples (500 and 650 °C-annealed samples cases).[27,31] For 500 °C-annealed sample, metallic Ni was present, whereas no metallic Ni could be seen after annealing 650 °C in XRD data. It is worth mentioning that using XPS only Ni oxide was seen for both samples (Fig. 3). These discrepancies between XRD and XPS analyses indicate that Ni_xP_y

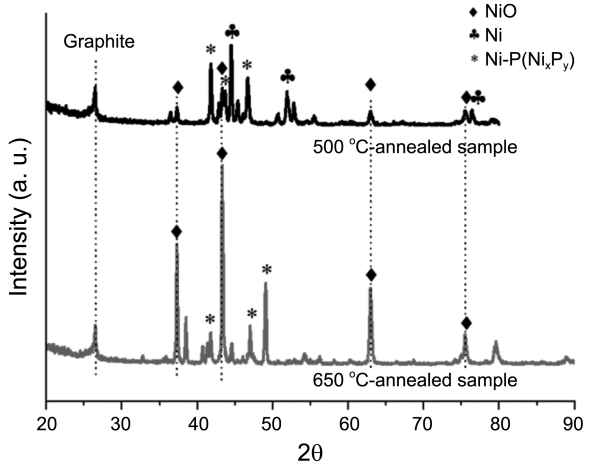

Figure 4. XRD patterns of 500 and 650 °C-annealed NiO filters are compared.

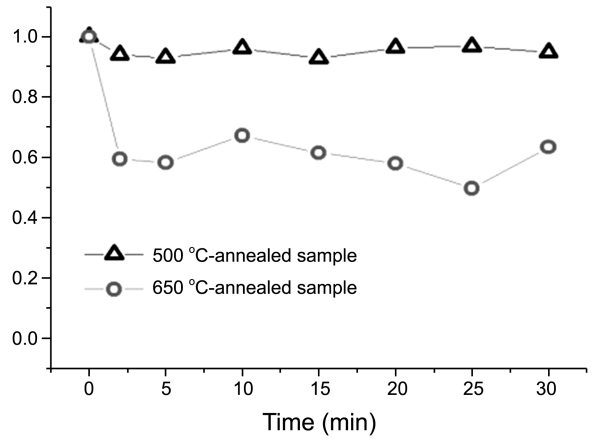

Figure 5. Changes in the relative partial pressure of toluene with respect to that of N_2 gas in the presence of 500 and 650 °C-annealed NiO filters are plotted as a function of reaction time.

states and metallic Ni did not exist on the surface or sub-surface region, but located in deeper layers. Note that only 4-5 nm from the very top surface can be detected in XPS, whereas bulk as well as surface properties can be observed in XRD. In both cases (500 and 650 °C-annealed samples), NiO, $Ni(OH)_2$ and Ni_xP_y phases co-existed in the deeper layers, whereas the surface region of the films consisted of NiO and $Ni(OH)_2$ species. The oxidic-Ni states had an amorphous structure when sample was annealed at 500 °C, whereas the amorphous NiO phases were converted to crystalline ones with increasing annealing temperature (650 °C). Metallic Ni existing in deeper layers after annealing at 500 °C should have been fully oxidized to NiO at 650 °C.

Chemical properties of these two NiO filters with meso (500 °C-annealed) and macro (650 °C-annealed) porous structures, respectively, were evaluated by toluene adsorption and oxidation experiments. In Figure 5, toluene adsorption capacities of both NiO filters (500 and 650 °C-annealed sample) were compared. Toluene adsorption experiments were performed in a vacuum condition (~8.0×10^{-8} torr) with a gas mixture of N_2 (80 mtorr) and toluene (5 mtorr) at room temperature. Decreases in the pressure ratio of toluene/N_2 due to toluene adsorption were observed for both cases of NiO filters annealed at either 500 or 650 °C. The amount of toluene adsorbed on the surface of 650 °C-annealed sample was larger than that of 500 °C-annealed one by a factor of ~8, indicating a higher density of active sites for toluene adsorption on the surface of 650 °C-annealed sample. This higher toluene adsorption capacity of 650 °C-annealed sample comparing to that of 500 °C-annealed one could be related to its unique morphology, a porous structure, which can result in a higher surface area (Fig. 1(f)).

Catalytic toluene oxidations as a function of reaction temperature over two differently annealed NiO filters were investigated using a flow type reactor (Fig. 6). The onset temperature of toluene oxidation using 500 °C-annealed sample was around 200 °C, which was significantly lower than that of 650 °C-annealed sample, *i.e.*, catalytic activity of 500 °C-annealed sample was much higher than that of 650

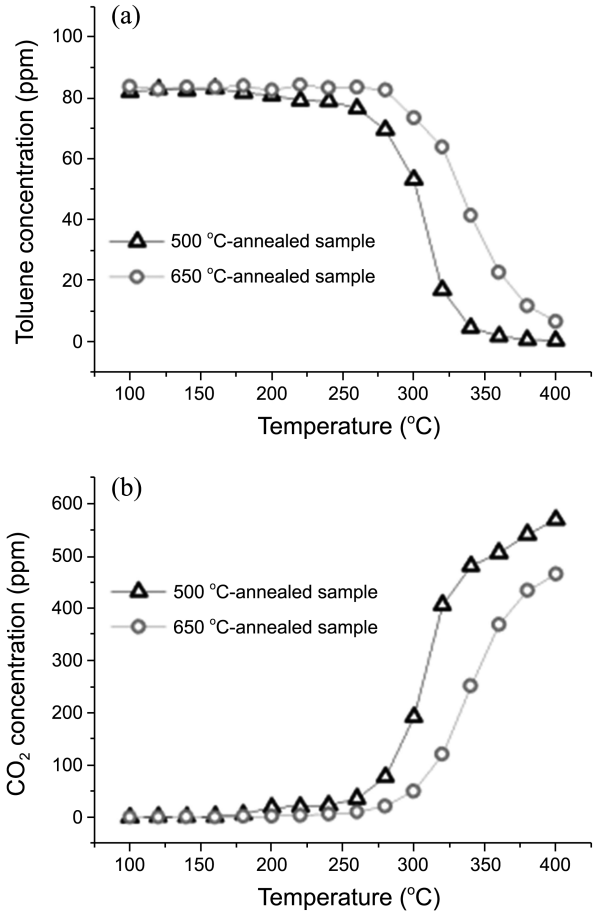

Figure 6. Changes in the (a) toluene and (b) CO_2 concentrations during toluene oxidation reactions in the presence of 500 and 650 °C-annealed NiO filters are shown as a function of reaction temperature.

Table 2. Results of toluene oxidation reactions with 500 and 650 °C-annealed NiO filters at 320 °C of reaction temperature are summarized and compared in terms of toluene removal ratios (%), turn over number (TON) and calculated activation energy

(At 320 °C)	500 °C annealed -Ni filter	650 °C annealed -Ni filter
Toluene Removal Ratio (%)	79.2	22.9
TON	43340.3	1587.1
Activation Energy (kJ/mol)	21.24	31.40

°C-annealed sample under our experimental condition. We calculated the activation energy of toluene oxidation using 500 and 650 °C-annealed sample respectively, using reactivity data at three different temperatures (300, 320, and 340 °C, Table 2). Moreover, catalytic behaviors of two NiO filters annealed at 500 and 650 °C, respectively, were summarized in terms of toluene removal ratio (%) and turn over number (TON) at 320 °C (Table 2). The activation energy of toluene oxidation using 500 °C-annealed NiO filter was 10 kJ/mol lower than that of reaction using 650 °C-annealed one. The toluene removal ratio on the surface of 500 °C-annealed NiO filter was larger than that on 650 °C-annealed

one; 79.2% (64 ppm) of toluene was oxidized on the surface of 500 °C-annealed NiO filter producing about 406.9 ppm of CO_2 at 320 °C, whereas 23% (18.4 ppm) of toluene was converted to about 120.3 ppm of CO_2 on that of 650 °C-annealed one at 320 °C under same experimental conditions. TON of toluene oxidation using 500 and 650 °C-annealed sample at 320 °C, was determined to be 43340 and 1587, respectively. Note that number of adsorption sites for each sample was determined from the experimental results of Figure 5, which was needed for determining TON of each catalyst. Interestingly, it is notable that 500 °C-annealed sample showed a higher catalytic reactivity (Fig. 6 and Table 2) despite of its lower toluene adsorption capacity comparing to that of 650 °C-annealed sample (Fig. 5). Our results of toluene adsorption and oxidation experiments with two NiO filters (500 and 650 °C-annealed ones) suggest that catalytic performances of NiO filters for toluene oxidation was not directly correlated to their numbers of surface toluene adsorption sites. Our result shows that the amorphous NiO surfaces of 500 °C-annealed sample should be more reactive for toluene oxidation than that of 650 °C-annealed sample with a higher crystallinity.

One may argue that the 650 °C-annleaed sample shows lower reactivity due to higher coverage of impurities on the surface as one can see in our XPS data in Table 1. However, it is worth mentioning that our previous studies on CO oxidation resulted in a superior catalytic activity for the NiO filter with a higher annealing temperature and higher porosity. Considering results of toluene adsorption experiments and CO oxidation using different NiO filters, 650 °C-annealed sample should have significantly more active sites.[32] NiO surface more reactive for CO oxidation turns out to be less reactive for toluene oxidation.[32]

Amorphous NiO surface can show higher concentrations of unsaturated surface sites, which can be catalytically reactive.[33] This could rationalize a higher reactivity of amorphous NiO surface for toluene oxidation. It is worth mentioning that metallic Ni was only present in deeper layers of 500 °C-annealed sample, not on the surface, and therefore role of metallic Ni for catalytic oxidation can be excluded.

Our result suggests that the porous structure with a higher surface area is not always beneficial for application in heterogeneous catalysis, and many other factors than surface area such as crystallinity should be taken into account for designing catalysts for various reactions.

Conclusion

Ni-P film with a thickness of 700-800 nm was deposited on carbon filter using an electroless plating method. SEM, XPS, and XRD analysis showed that two different NiO structures (amorphous NiO films with mesoporous surface and crystalline ones with macroporous structure) could be prepared by post-annealing of as-prepared Ni-P films at 500 and 650 °C, respectively. Chemical properties of two NiO filters were investigated by toluene adsorption and catalytic toluene oxidation experiments. The 650 °C-annealed NiO filter with a macroporous surface structure had a higher toluene adsorption capacity than 500 °C-annealed one with a mesoporous surface structure by a factor of ~8. However, 500 °C-annealed Ni films showed rather higher catalytic reactivity with respect to that of 650 °C-annealed one despite of its lower toluene adsorption capacity. XRD and XPS analysis suggested that amorphous NiO was more reactive for toluene oxidation than crystalline NiO.

Acknowledgments. This research was supported by a grant from the Fundamental R & D Program for Core Technology of Materials funded by the Ministry of Knowledge Economy, Republic of Korea.

References

1. Browning, E. *Toxicity and Metabolism of Industrial Solvents*; Elsevier Publishing Company: Amsterdam, Netherland, 1965.
2. Busca, G.; Berardinelli, S.; Resini, C.; Arrighi, L. *J. Hazard. Mater.* **2008**, *160*, 265.
3. Mudliar, S.; Giri, B.; Padoley, K.; Satpute, D.; Dixit, R.; Bhatt, P.; Pandey, R.; Juwarkar, A.; Vaidya, A. *J. Environ. Manage.* **2010**, *91*, 1039.
4. Lewis, A. C.; Carslaw, N.; Marriott, P. J.; Kinghorn, R. M.; Morrison, P.; Lee, A. L.; Bartle, K. D.; Pilling, M. J. *Nature* **2000**, 405, 778.
5. Tsou, J.; Magnoux, P.; Guisnet, M.; Órfão, J. J. M.; Figueiredo, J. L. *Appl. Catal. B: Environ.* **2005**, *57*, 117.
6. Walerczyk, W.; Zawadzki, M. *Catal. Today* **2011**, *176*, 159.
7. He, C.; Li, J.; Zhang, X.; Yin, L.; Chen, J.; Gao, S. *Chem. Eng. J.* **2012**, *180*, 46.
8. Sun, H.; Chen, S.; Wang, P.; Quan, X. *Chem. Eng. J.* **2011**, *178*, 191.
9. Scirè, S.; Minicò, S.; Crisafulli, C.; Satriano, C.; Pistone, A. *Appl. Catal. B: Environ.* **2003**, 40 , 43.
10. Aguero, F. N.; Barbero, B. P.; Almeida, L. C.; Montes, M.; Cadús, L. E. *Chem. Eng. J.* **2011**, *166*, 218.
11. Somekawa, S.; Hagiwara, T.; Fujii, K.; Kojima, M.; Shinoda, T.; Takanabe, K.; Domen, K. *Appl. Catal. A: Gen.* **2011**, *409-410*, 209.
12. Kovanda, F.; Jirátová, K. *Catal. Today* **2011**, *176*, 110.
13. Kim, K.-D.; Nam, J. W.; Seo, H. O.; Kim, Y. D.; Lim, D. C. *J. Phys. Chem. C* **2011**, *115*, 22954.
14. Grbic, B.; Radic, N.; Terlecki-Baricevic, A. *Appl. Catal. B: Environ.* **2004**, *50*, 161.
15. Garcia, T.; Agouram, S.; Sánchez-Royo, J. F.; Murillo, R.; Mastral, A. M.; Aranda, A.; Vázquez, I.; Dejoz, A.; Solsona, B. *Appl. Catal. A: Gen.* **2010**, *386*, 16.
16. de Rivas, B.; Gutiérrez-Ortiz, J. I.; López-Fonseca, R.; González-Velasco, J. R. *Appl. Catal. A: Gen.* **2006**, *314*, 54.
17. Perez-Alonso, F. J.; Melián-Cabrera, I.; Granados, M. L.; Kapteijn, F.; Fierro, J. L. G. *J. Catal.* **2006**, *239*, 340.
18. Bueno-López, A.; Krishna, K.; Makkee, M.; Moulijn, J. A. *Catal. Lett.* **2005**, *99*, 203.
19. Lahousse, C.; Bernier, A.; Grange, P.; Delmon, B.; Papaefthimiou, P.; Ioannides, T.; Verykios, X. *J. Catal.* **1998**, *178*, 214.
20. Peng, G.; Merte, L. R.; Knudsen, J.; Vang, R. T.; Lægsgaard, E.; Besenbacher, F.; Mavrikakis, M. *J. Phys. Chem. C* **2010**, *114*, 21579.
21. Knudsen, J.; Merte, L. R.; Peng, G.; Vang, R. T.; Resta, A.; Lægsgaard, E.; Andersen, J. N.; Mavrikakis, M.; Besenbacher, F. *ACS. Nano* **2010**, *4*, 4380.
22. Lee, H. J.; Seo, H. O.; Kim, D. W.; Kim, K.-D.; Luo, Y.; Lim, D. C.; Ju, H.; Kim, J. W.; Lee, J.; Kim, Y. D. *Chem. Commun.* **2011**, *47*, 5605.
23. Greiner, M. T.; Helander, M. G.; Wang, Z.-B.; Tang, W.-M.; Lu, Z.-H. *J. Phys. Chem. C* **2010**, *114*, 19777.

24. Moulder, J. F.; Stickle, W. F.; Sobol, P. E.; Bomben, K. D. *Handbook of X-ray Photoelectron Spectroscopy*; Chastain, J., King, R. C., Jr., Eds.; Physical Eletronics, Inc.: Minnesota, U.S.A., 1995.
25. Elsener, B.; Atzei, D.; Krolikowski, A.; Albertini, V. R.; Sadun, C.; Caminiti, R.; Rossi, A. *Chem. Mater.* **2004**, *16*, 4216.
26. Ochs, D.; Dieckhoff, S.; Cord, B. *Surf. Interface. Anal.* **2000**, *30*, 12.
27. Cecilia, J. A.; Infantes-Molina, A.; Rodríguez-Castellón, E.; Jiménez-López, A. *J. Catal.* **2009**, *263*, 4.
28. Rengifo-Herrera, J. A.; Blanco, M. N.; Pizzio, L. R. *Appl. Catal. B: Environ.* **2011**, *110*, 126.
29. Zhang, H. J.; Chen, Z. Q.; Wang, S. J. *J. Chem. Phys.* **2012**, *136*, 034701.
30. Castro-Hurtado, I.; Herrán, J.; Mandayo, G. G.; Castaño, E. *Thin. Solid Films* **2011**, *520*, 947.
31. Loboué, H.; Guillot-Deudon, C.; Popa, A. F.; Lafond, A.; Rebours, B.; Pichon, C.; Cseri, T.; Berhault, G.; Geantet, C. *Catal. Today* **2008**, *130*, 63.
32. Seo, H. O.; Nam, J. W.; Kim, K.-D.; Sim, J. K.; Kim, Y. D.; Lim, D. C. *J. Mol. Catal. A* **2012**, *361-362*, 45.
33. Deng, J.-F.; Li, H.; Wang, W. *Catal. Today* **1999**, *51*, 113.